Int. J. Nano Dimens., 10 (4): 320-329, Autumn 2019

ORIGINAL ARTICLE

Biosynthesized Zinc Oxide nanoparticles control the growth of *Aspergillus flavus* and its aflatoxin production

Priti Kumari [1], Harish Kumar [2], Jainendra Kumar [2], Mohammad Sohail [3], Krisn Pratap Singh [3], and Kamal Prasad [4,*]

[1] *Aryabhatta Centre for Nanoscience and Nanotechnology, Aryabhatta Knowledge University, Patna, 800001, India.*

[2] *Department of Botany and Biotechnology, College of Commerce, Arts and Science, Patna, 800020, India.*

[3] *University Department of Zoology, Vinoba Bhave University, Hazaribag, 825301, India.*

[4] *University Department of Physics, T.M. Bhagalpur University, Bhagalpur, 812007, India.*

Received 08 April 2019; revised 07 August 2019; accepted 09 August 2019; available online 10 August 2019

Abstract

The infection of *Aspergillus flavus* and its aflatoxin production pose a severe threat to humans, animals as well as plants life. Their inhibition using green techniques are considered as one of the important challenges. The present study outlines the antifungal activity of the ZnO nanoparticles (NPs) synthesized from lemongrass leaf extract and their effect on the mycelial growth of *Aspergillus flavus* and its aflatoxins production. The qualitative and quantitative analyses of aflatoxins were determined, respectively using thin-layer chromatography and spectrophotometric methods. The X-ray diffraction as well as scanning and transmission electron microscopy studies indicated the formations of hexagonal ZnO NPs having the sizes ranged between 7 and 14 nm. FTIR spectrum confirmed the formation of ZnO NPs. The ZnO NPs displayed 92.25% inhibition of the growth of *A. flavus* and 100% inhibition of the aflatoxins production at the concentrations of 200 µl/mL and 150 µl/mL respectively. The present biosynthetic method is a simple, cost-effective, eco-friendly, high yield, green and handy protocol capable of synthesizing ZnO NPs, which might have accomplished due to the activities of plant metabolites and phytochemicals available in the lemongrass leaves parenchyma. This study revealed that ZnO NPs have the potential to forbid the growth of *A. flavus* and its aflatoxins production. Hence, ZnO NPs could be used in the plant protection and as a preservative for safe storage of food commodities to prevent *A. flavus* contamination and aflatoxins poisoning in coming future.

Keywords: *Aflatoxin; Aspergillus Flavus; Green Synthesis; Lemongrass; Plant Fungal Pathogens; Plant Protection; ZnO Nanoparticles*

How to cite this article

Kumari P, Kumar H, Kumar I, Sohail M, Pratap Singh K, Prasad K. Biosynthesized Zinc Oxide nanoparticles control the growth of Aspergillus flavus and its aflatoxin production. Int. J. Nano Dimens., 2019; 10 (4): 320-329.

INTRODUCTION

Aspergillus flavus – an aflatoxin producing fungus, is a harmful mold which spoils various food and/or agriculture items such as cotton corn, peanuts, seeds, and tree nuts [1]. It affects 25-40% of agricultural products of the raw world [2] and causes liver cancer as well as aspergillosis in humans and animals including livestock. The secretion of various enzymes like pectinase, cellulose, protease, and amylase may cause damage to the plant tissues. Also, this mold produces aflatoxins that are considered as highly toxigenic, mutagenic, carcinogenic and teratogenic [3]. International Agency for Research on Cancer (IARC) has listed aflatoxins as "Class 1 Human Carcinogen" [4]. Aflatoxins are also considered as harmful to plant growth because they show inhibitory effect on various processes of plants such as during root elongation, seedling growth, seed germination,

* Corresponding Author Email: *prasad_k@tmbuniv.ac.in*
k.prasad65@gmail.com

chlorophyll synthesis and production of some useful enzymes [5, 6]. It is observed that the tropical, as well as sub-tropical countries are very much prone to the contamination of aflatoxins contamination because of their harsh (hot as well as humid) climatic circumstances which are benign for fungus growth and mycotoxins synthesis [2]. It is seen that the prolong storage of crops and food materials cause oxidative stress and generation of free-radical [7]. Both oxidative stress and free radical generation promote the biosynthesis of aflatoxins by *A. flavus* [8]. Spreading of the infection of *A. flavus* along with its aflatoxin in both human and animal life has imposed a challenging scenario around the world. It is, therefore, needed to evolve appropriate methods to overcome the aflatoxin contamination problems especially towards the safety of food commodities utilizing green technology.

In recent years, nanomedicines are considered a better option for the remedy of various types of diseases including the diseases caused by fungus. As a result, various functionalized nanoparticles are being utilized to wipe out fungal infections [9-13]. Further, zinc oxide (ZnO), an inorganic compound, has received remarkable scientific and technological attention due to its antibacterial [14], antifungal [15,16], antioxidant [17], anticancer [18-20], antiangiogenic and antiapoptotic [21] activities. Also, it is being utilized in sunscreen, cosmetics, agriculture, optoelectronics, solar cells, piezoelectric, sensor, and water remediation [22]. ZnO nanoparticles (NPs) is a semiconductor material having an optical band gap of 3.37 eV which is like TiO_2 (3.23 eV) nanoparticles [23]. ZnO NPs is listed as a very low/non-toxic material which is being used for the development of different products like moisturizers, lip products, mineral make-up base, hand-cream, face-powder, ointments in bacterial as well as fungal infections. It has a higher surface area, chemical reactivity, adsorption capacity, *etc*. compared to the bulk ZnO. These factors have led ZnO NPs to interact adroitly with biosystems to generate ROS on the surface of the particles [24, 25]. Besides, the lemongrass (*Cymbopogon citrates*) is a common medicinal plant which is known for its antimicrobial properties [26, 27]. Accordingly, in this study, biocompatible ZnO NPs have been synthesized from the lemongrass leaves using green chemistry approach and characterized by X-ray diffraction (XRD), dynamic light scattering (DLS), scanning and transmission electron microscopy studies. Also, the possible biosynthetic mechanism for ZnO NPs formation using *Cymbopogon citrates* has been discussed. Most importantly, the antifungal and anti-aflatoxigenic activities of as-synthesized ZnO NPs against the *A. flavus*, have been undertaken to access their utilization as a green alternative (as an antifungal agent) in food as well as agriculture sciences.

MATERIALS AND METHODS

Test materials pathogen

Aflatoxigenic strains of *Aspergillus flavus* were inoculated on freshly prepared Czapek-Dox Agar media (CDA) and Potato Dextrose Agar Media (PDA) and were incubated at 28 °C for 10 days.

Biosynthesis of ZnO nanoparticles using lemongrass leaves

Freshly collected leaves of lemongrass were rinsed thoroughly using de-ionized water and allowed to dry in an airy atmosphere and then cut into fine pieces. The 10 g of which was then mixed with 100 mL of 50 % acetone in a conical flask (250 mL) and the mixture was then allowed to boil for 20 min at 60ºC on water bath before decanting till the colour changes from clear transparent to deep green. The extract was then filtered utilizing a filter paper (Whatman no. 1). Thereafter, 10 mM aqueous Analytical reagent grade $ZnCl_2$ solution was added to lemongrass leaf extract and the solution was placed in an orbital shaker at 60ºC which was heated so that the solution appears to be hazy (starch like) and white mass starts deposited at the bottom of the flask. This was perceived as the initiation of nano-transformation. Thereafter, the flask was incubated for another four hours in the laboratory ambiance till duck white fluffy mass of ZnO NPs settles at the base and leaves a clear transparent supernatant at the top. The obtained ZnO NPs from the solution was washed thrice with deionized water by repeatedly get centrifuged at 5000 rpm for about 10 min to remove the soluble biomolecules like proteins as well as secondary metabolites. The water suspended ZnO NPs were dried at 60 ^oC in a hot air oven and the pellet was stored at 4^oC for further use.

Physical characterizations

To ascertain the formation of ZnO NPs and to know the unit cell parameters, X-ray diffraction study was undertaken with a PANalytical's X'Pert

PRO X-ray diffractometer. The CuK_{α} radiation (λ = 1.5406Å) was used over Bragg angles (2θ) between 20° and 80°. The size and shape of ZnO NPs were evaluated through Carl Zeiss Microscopy Ltd., UK makes scanning electron microscope (EVO 18). The TEM picture of ZnO NPs was collected by a Bruker transmission electron microscope. The particle sizes were estimated from software (*Image J*) considering 20 particles. The distribution of particle sizes of ZnO NPs was confirmed using a dynamic light scattering particle size cum zeta potential analyser (Micromeritics Instruments Corp., USA). The Fourier Transformed Infrared (FTIR) spectrum of ZnO NPs was obtained using FTIR spectrophotometer (PerkinElmer, UK) in transmission mode in the wavelength range of 4500-375 cm^{-1}.

Biological characterizations

Antifungal activity

To assess the antifungal activity of the zinc oxide nanoparticles, agar plate diffusion method was employed in which different concentrations of the ZnO NPs (150, 200 and 250 µl/mL) were dissolved in 20 mL of PDA medium in different Petri plates. Afterward, freshly prepared fungal disc (5 mm diameter) of *Aspergillus flavus* was inoculated at the centre of each plate containing a different concentration of ZnO NPs. One Petri plate was used as a control, in which ZnO NPs were not added. Thereafter, all Petri plates were incubated for 72 hours at 28 °C. The diameter (in cm) of the mold growth, in each Petri plate, was measured. The inhibition of growth (%) of *A. flavus* was calculated from the formula: $Inhibition\ of\ \ growth\ of\ \ test\ fungi = [(D_C - D_T)/D_C] \times 100\%.$ Here, D_C and D_T are, respectively, the average increase in mycelial growth in the control and the test samples.

Thin Layer Chromatography (TLC)

The freshly prepared Czapek Dox Broth (CDB) medium was transferred into different conical flasks (25 mL in each flask) of 100 mL capacity to analyse the anti-aflatoxigenic activity of ZnO NPs. The requisite amount of the ZnO NPs were dissolved in 25 mL of CDB medium in each flask to get final concentration of 50µl, 100µl, 150µl, 200µl and 250µl/mL separately, and subsequently a fungal disc of *Aspergillus flavus* (5 mm diameter) was inoculated into each flask containing the specified concentrations of the ZnO NPs. A flask was used as a control, in which ZnO NPs were not added. Afterward, all flasks were incubated for 10 days at 28°C. The *A. flavus* mycelium of each flask was then filtered using Whatman no.1 filter paper which was autoclaved to destroy the harmful spores of the mold and the autoclaved mycelium was dried for 12 hours at 80°C in an oven. The extraction of the filtrate was carried out with 25 mL chloroform. The extracted and purified treated and control samples of aflatoxins were spotted on MN-KIESEFELL G-HR thin-layer chromatography (Machery, Nage and Company Duran F.R.G.) using a Diesaga micro-syringe (Heidelberg F.R.G.) with acetone: chloroform (1:9) as developing solvents. The amount of aflatoxin was calculated by the comparison of standard spots and the formula adopted by the modification of Pons method [28].

Quantitative estimation of aflatoxin using enzyme-linked immunosorbent assays (ELISA)

Further to more precision and substantiate the thin-layer chromatography (TLC) observation in control and nanoparticles treated samples, we used a more specific and sensitive method for estimating aflatoxin, based on competitive enzyme-linked immunosorbent assays (ELISA). We used commercially available solid-phase direct competitive enzyme immunoassay based Total Aflatoxin ELISA kit from Sigma (SE120006) following standard sampling and test procedure according to the manufacturer's instructions. The optical densities were measured by a microplate reader set to 450 nm wavelengths and the arithmetic mean of the duplicate samples was considered for the analysis.

RESULT AND DISCUSSION

Fig. 1 depicts the XRD data obtained for ZnO NPs synthesized from lemongrass leaves using acetone extract along with the peak positions as given in the standard literature PDF No. #89-0510. The clear-cut broadening of XRD peaks indicated the formations of small-sized particles and absence of extra diffraction peaks suggested that ZnO NPs are free from any kind of impurities. The Bragg reflections (2ϑ) of various lattice-planes of Wurtzite hexagonal ZnO were identified using the *Full Prof* software. Also, the observed XRD peaks of ZnO NPs were found identical to that of bulk ZnO. The unit cell parameters as obtained from the analysis are *a* = 3.2508 Å and *c* = 5.2087 Å for the acetone-mediated synthesis of ZnO NPs

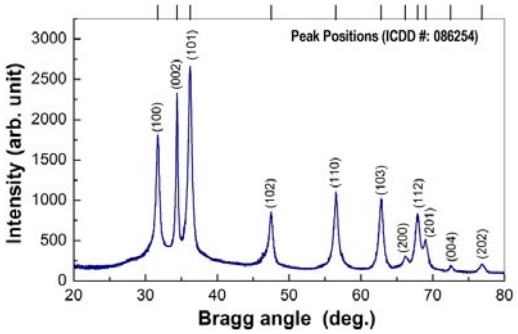

Fig. 1. X-ray diffractogram of ZnO NPs at room temperature synthesized using acetone extract of lemon grass (Cymbopogon citrates) leaves with Zn^{2+} ions.

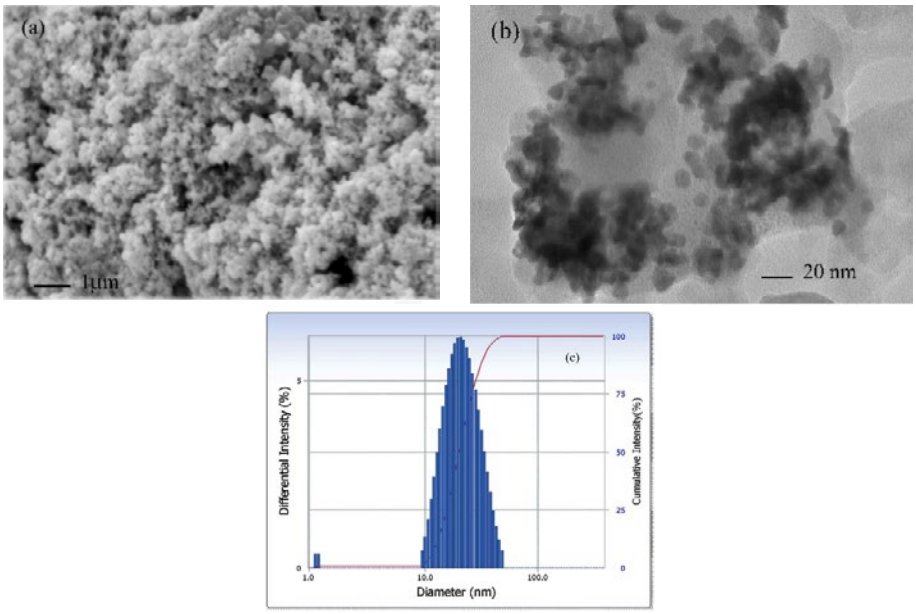

Fig. 2. (a) SEM, (b) TEM images and (c) particle size distribution of ZnO NPs synthesized by Zn^{2+} ions using lemongrass leaves broth.

with space group *P*6/*mmm* (191), which agree excellently well with the literature (PDF No. #89-0510) [29-31]. The direct cell volume was obtained to be ~47.67 Å^3. The average particle sizes (*D*), as well as lattice strain ($\Delta\xi/\xi$) of prepared ZnO NPs, were approximated by evaluating the XRD peaks' broadening, utilizing Williamson and Hall method $B\cos\theta = (K\lambda/D) + 2(\Delta\xi/\xi)\sin\theta$, here *B* and *K* are the XRD peak width at the half intensity and the Scherrer constant (0.89) respectively. Further, the terms *Kλ*/*D* and $2(\Delta\xi/\xi)\sin\theta$ respectively represent the Scherrer particle size and the strain broadening. The value of *B* was estimated using a Lorentzian model. The average particle size, as well as lattice strain of ZnO NPs, was found to be ~10 nm and ~0.003 using the linear least-square fitting of *B*cosϑ-sinϑ data. Such a small value of lattice strain is due to the reason that the nanoparticles synthetic protocol as adopted is considered as natural (biological synthesis) one [32] in which the constraint imposed during the formations of nanoparticles is negligibly small compared to extensive ball milling, strained layer growth, *etc*. techniques. Hence, the current biosynthetic method is capable of synthesizing ZnO NPs, which might have been resulted due to the activities of different plant metabolites as well as the presence of different phytochemicals in the lemongrass leaves parenchyma.

Fig. 2 (a), (b), and (c), respectively illustrate the SEM and TEM images and the particle size distribution (DLS) of the biosynthesized ZnO NPs. The SEM micrograph indicates the formation of small-sized particles in the little nanometer range.

This observation has been well supported by the TEM micrograph, which ensures the formations of ZnO NPs which are nearly spherical with the sizes ranging between 7 and 14 nm with very few agglomerations. This result is in wonderful compliance with the experimental DLS data (Fig. 2c). The differences in the sizes of biosynthesized nanoparticles may probably be because of the reality that the nanoparticles have been formed at different times and agglomerations due to the high surface energy. Besides, it is found that the average size of particles estimated using Williamson and Hall method to be in nearly good compliance with the sizes estimated by SEM, TEM as well as DLS results.

Fig. 3 (a) depicts the biosynthetic mechanism for the formations of ZnO NPs using *Cymbopogon citrates* (lemongrass) which are inundated with different metabolites and aroma. It is noticed that the extract of lemongrass leaf contains different metabolites such as flavonoids, alkaloids, carbohydrates, glycosides, saponins, tannins, anthraquinones, steroids, phenols, *etc*. Besides, the compounds such as methylheptenone, fumesol, furfurol, isopulegol, p-coumaric acid, isovaleranic aldehyde, L-linanool, ndecyclic aldehyde, terpineone, valeric esters, etc. are also present in lemongrass leaf [33]. Also, noticed that among the flavonoids, quercetin and kaempferol glycosides are the main content of lemongrass, which is oxidoreductive labile molecules. Further, citral, geranial, myrcene, limonene, nerol, geraniol, citronellol, burneol, neral, α-terpineol, elemicin, apigenin, chlorogenic acid, caffeic acid, kaempferol, quercetin, geranyl acetate, and luteolin are present in the form of volatile oil [34]. These are the well-defined and well-developed metabolic machinery. The process of nano-transformation, in the present case, could be culminated because of the tautomerization of quercetin (Fig. 3a). It is believed that the existence of –OH (enol group) in quercetin can tautomerize in –C=O (keto group) [29, 30, 35]. While keto form of quercetin under an oxidizing environment, due to a low pH

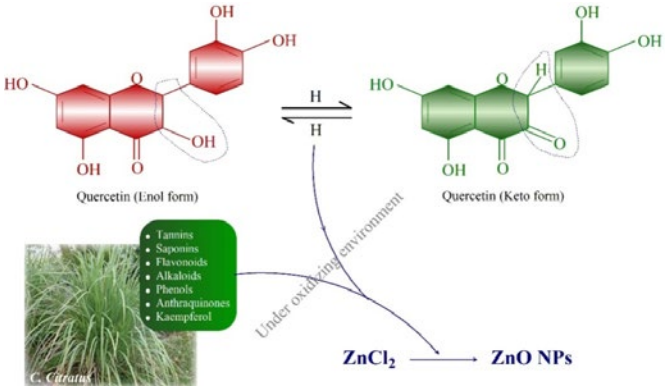

Fig. 3a. Schematics for the biosynthesis of ZnO nanoparticles using lemongrass leaves broth.

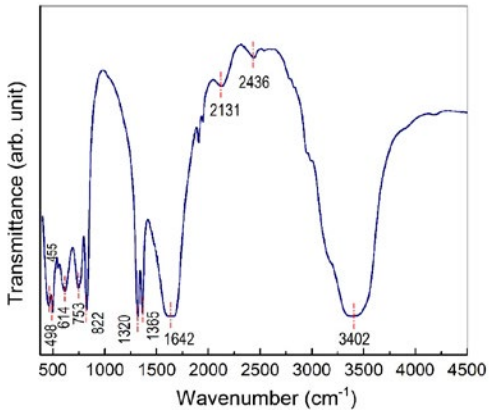

Fig. 3b. FTIR spectrum of ZnO nanoparticles synthesized using lemongrass leaves broth.

condition, might be transformed into enol form of quercetin. A rapid nano-transformation from the extract is intriguing a redial-tautomerization [36]. Further, no shift in pH value was observed and/or persuaded in the extracts, however upon gentle warming and subsequent incubation might have activated the quercetin congeners which lead to the reduction in particle sizes and the formations of coalescent clusters which act as capping agent. Fig. 3(b) illustrates the FTIR spectrum of the ZnO NPs. The intense broad absorption peak at 3402 cm^{-1} is correlative to hydrogen bonded O-H stretching of alcohols and phenols. The peaks at 2436 cm^{-1} and 2131 cm^{-1} may, respectively be due to the presence of CO_2 and –C=C– stretching. The peak at 1642 cm^{-1} is owing to the –HC=CH– group while the peaks 1365 cm^{-1} and 1320 cm^{-1} may, respectively correspond to C–C and C–H bonding. The C=C as well as C–N stretching could be seen at the peak positions 822 and 753 cm^{-1}. The presence of few peaks between 455 to 614 cm^{-1} may correspond to the formation of Zn–O bond. The FTIR results could confirm that the presence of the functional groups in the extract serves as the reducing as well as capping agent for ZnO NPs.

The antifungal activities of acetone mediated

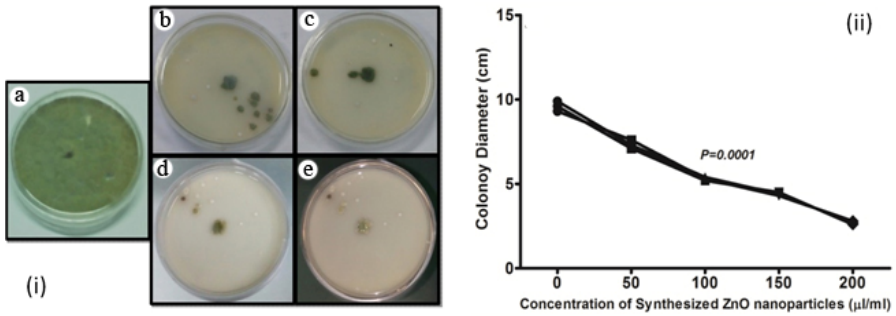

Fig. 4. (i) Concentration dependence ZnO NPs on the growth of Aspergillus flavus (a) untreated culture, (b) treated with 50 µl/mL, (c) treated with 100 µl/mL, (d) treated with 150 µl/mL and (e) treated with 200 µl/mL and (ii) Reduction trend of colony density.
(The data represent the triplicate measurements per concentration. The statistical analysis was calculated using 2-way ANOVA comparing between the stratified concentration of nanoparticles group and untreated group. The significance were considered P ≤ 0.05 using GraphPad Prism version 5.0).

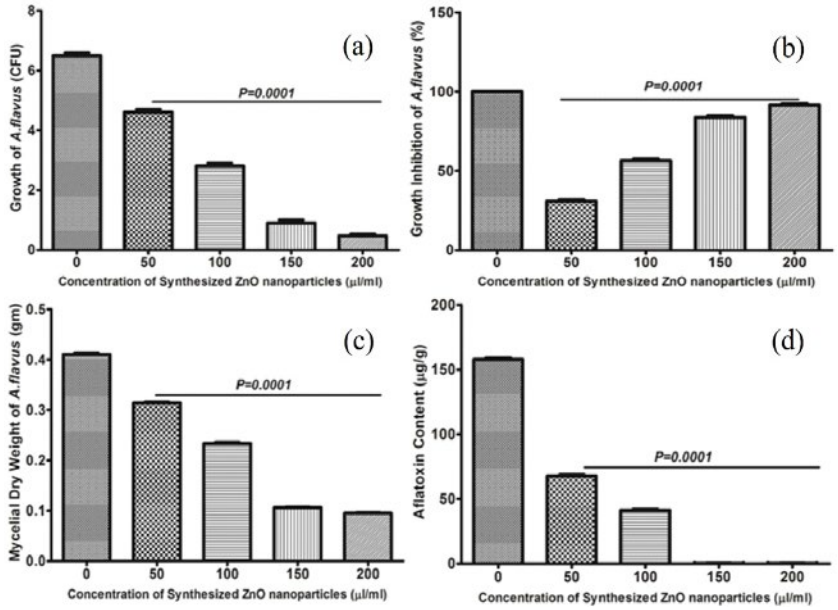

Fig. 5. Concentration dependence of ZnO NPs on the (a) growth of Aspergillus flavus, (b) growth inhibition of A. flavus, (c) mycelial dry weight and (d) aflatoxin content.
(The data represent the Mean ± SD of triplicate experiment having N = 3 per bar. The statistical analysis was calculated using 2-way ANOVA comparing between the stratified concentration of nanoparticles group and untreated group. The significance were considered P ≤ 0.05 using GraphPad Prism version 5.0).

lemongrass leaves extract synthesized ZnO NPs over the growth of *Aspergillus flavus* at different concentrations (untreated culture, treated with 50, 100, 150, and 200 µl/mL) are presented in Fig. 4(i). The antifungal activities of ZnO NPs could be seen which opposes the growth of *Aspergillus flavus* in a dose-depended manner. A reduction trend of colony density could easily be seen on the plates and a quantitate data of which has been illustrated in Fig. 4(ii) in support of these observations. The untreated sample (control) displayed the production of *A. flavus* (Fig. 4(i) a), but the ZnO NPs treated samples showed 31.9% (Fig. 4(i) b), 57.6% (Fig. 4(i) c), 84.9% (Fig. 4(i) d) and 92.25% (Fig. 4(i)e) inhibition of the growth of these molds at the concentrations of 50 µl/mL, 100 µl/mL, 150 µl/mL and 200 µl/mL, respectively.

Fig. 5 shows the anti-aflatoxigenic effect of ZnO NPs. The result of anti-aflatoxigenic activity exhibited that ZnO NPs has the potential to inhibit the aflatoxins biosynthesis from the toxigenic strain of *Aspergillus flavus.* The ZnO NPs inhibited 100% aflatoxins biosynthesis at 150 µl/mL concentration and above. The growth of *A. flavus* and its aflatoxins biosynthesis were recorded to decrease with the increment in the ZnO NPs concentration. Also, it was noticed that the decrement in mycelial weight of *A. flavus* leads to a reduction in aflatoxins production. Therefore, the mycelial growth of this mold must be arrested below the threshold value to inhibit the biosynthesis of aflatoxins.

Aspergillus flavus is a deadly pathogen due to the production of highly carcinogenic aflatoxins. There is a direct correlation between aflatoxin intake and the occurrence of liver cancer. Outbreaks of aflatoxins contamination food drew public attention to food safety. Aflatoxigenic *A. flavus* are found in most of the feed samples and produces aflatoxin. International Agency for Research on Cancer (IARC) has listed aflatoxins as highly carcinogen secondary metabolites. In the present work, we quantified the aflatoxin content through TLC in a stratified group of samples *i.e*. in the crude fungal colony (Fig. 6a, Lane-1), mycelial extract (Fig. 6a, Lane-2), and solvent extracted (Fig. 6a, Lane-3). It can be seen that the untreated sample (control) illustrated the bands of aflatoxins on TLC plate (Fig. 6a), whereas the ZnO NPs treated sample did not display the bands of aflatoxins onto the TLC plate (Fig. 6b). Hence, it was found difficult to quantify the ZnO NPs concentration-dependent treatment on the aflatoxin reduction due to less sensitivity and limitations of the TLC method (Fig. 6b). The mean aflatoxin content as found to be 159.6 µg/g, 155.3 µg/g and 159.7 µg/g; respectively and are depicted in Fig. 6c. To optimize the actual quantification, to access the impact of treated nanoparticles on the reduction of aflatoxin

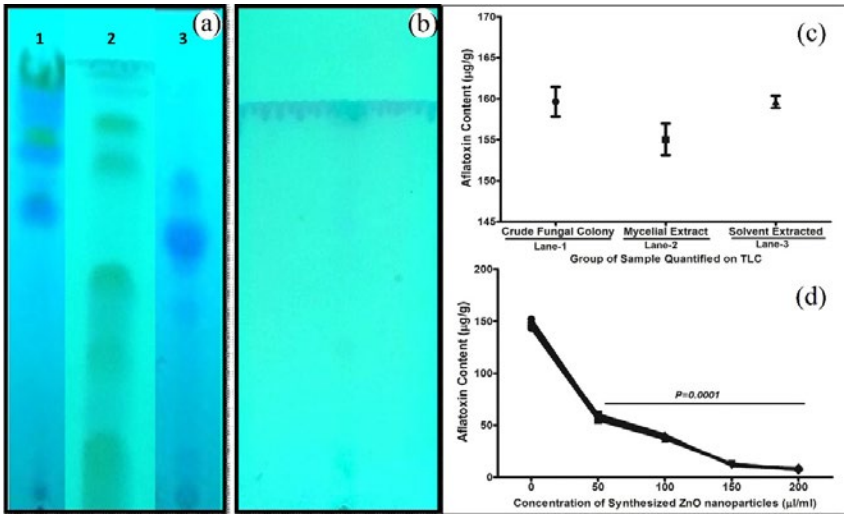

Fig. 6. Qualitative and quantitative effect of synthesized ZnO NPs on aflatoxin production by Aspergillus flavus (a) qualitative resolution of fungal colony (Lane-1), mycelial extract (Lane-2) and solvent extracted aflatoxin (Lane-3) on TLC plate; (b) resolution of nanoparticles treated with 50µl/mL, 100µl/ml, 150µl/mL, and with 200 µl/mL on TLC plate; (c) quantification of aflatoxin content in Lane-1, Lane-2 and Lane-3 as resolved in panel A and (d) total aflatoxin quantification by ELISA after treatment with stratified synthesized ZnO nanoparticles. The data represent the triplicate measurements per concentration.
(The statistical analysis was calculated using 2-way ANOVA comparing between the stratified concentration of nanoparticles group and untreated group. The significance were considered P ≤ 0.05 using GraphPad Prism version 5.0).

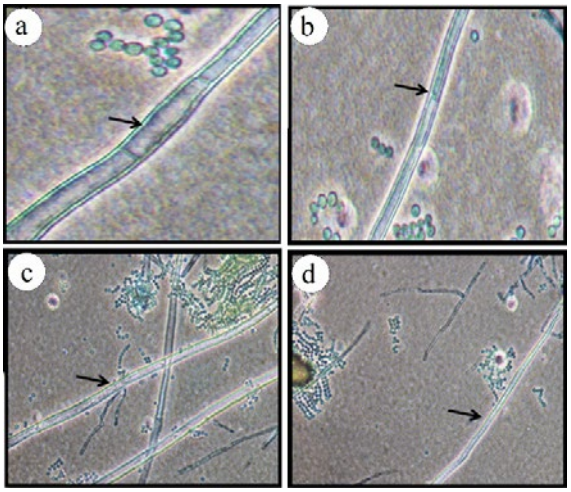

Fig. 7. Concentration-dependent effect of biosynthesized ZnO nanoparticles on the hyphal structure of Aspergillus flavus (a) Untreated (b) Treated with 50 µl/mL (c) Treated with 150 µl/mL, and (d) Treated with 200 µl/mL.

content, and to substantiate the findings of TLC, a more sophisticated and sensitive ELISA method of quantification was employed. ELISA provides a simple, rapid, and high-throughput detection of aflatoxins. We evaluated the samples treated with nanoparticles in stratified concentration *i.e*. 50 µl/mL, 100 µl/mL, 150 µl/mL, and 200 µl/mL as compared to control group and observed mean aflatoxin content 57.6 µg/g, 38.9 µg/g, 12.1 µg/g, and 7.7 µg/g; respectively in treated samples as compared to 147.5 µg/g in control group, as shown in Fig. 6d and differences between the ZnO NPs treated and control group were observed to be highly significant ($p = 0.0001$). These results showed the anti-aflatoxigenic effect of the lemongrass negotiated ZnO NPs. The result of anti-aflatoxigenic activity exhibited that ZnO NPs can inhibit the aflatoxins biosynthesis from the toxigenic strain of *Aspergillus flavus.* Besides, the ZnO NPs exhibited 100% inhibition of aflatoxins biosynthesis at 150 µl/mL. The growth of *A. flavus* and its aflatoxins biosynthesis were recorded to decrease while the increment in the concentration of the ZnO NPs. Also, it was noticed that the decrease in the mycelial weight of *A. flavus* leads to a reduction in aflatoxins production. Therefore, the mycelial growth of this mold must be arrested below the threshold value to inhibit the biosynthesis of aflatoxins.

Microscopic studies revealed that ZnO NPs can prevent the hyphal growth of *Aspergillus flavus* which solely dependent upon the applied doses (Fig. 7a-d). When 50 µl/mL ZnO NPs was used to treat *Aspergillus flavus* then the thickness of hypha was seen to decrease (Fig. 7a) than ZnO NPs untreated *A. flavus* (Fig. 7b) and thickness of hypha were recorded to decrease with the increment in the ZnO NPs concentration and finally at 200 µl/mL, very thin hypha was observed (Fig. 7d) in comparison to nanoparticle untreated sample. Hence, this experiment suggests that ZnO NPs reduces the capability of hypha formation of *A. flavus* which solely depends on the dose. Aflatoxins concentration was also recorded to decrease with the increment in the ZnO NPs concentration and finally, at 200 µl/mL, aflatoxins were not detected during spectrophotometry study (quantitative) (Fig 7d). These data support the observations of Guzmán-de-Peña and Ruiz-Herrera [36], who reported that there exists a direct relationship between hypha, mycelium and aflatoxins production. Hopwood [38] also suggested that hypha formation is linked with aflatoxins production. Other researchers, Van Rensburg *et al.* [39], and Doyle and Marth [40], hypothesized that breakage or lysis of hypha decreases the production of aflatoxins because aflatoxins degrading factors are intracellular constituents of hypha and when the integrity of hypha is disrupted then these aflatoxins degrading factors release into the medium, and degrade the production of aflatoxins.

This study revealed that ZnO NPs possess the excellent capability to detain the growth of *A. flavus* and production of aflatoxins. Hence, present work might be a step towards possible utilization

of ZnO NPs in the plant protection and as an antifungal agent especially against aflatoxins and/ or aspergillosis and may act as a preservative for safe-storage of food merchandise to forbid from the contamination of *A*. *flavus* and the aflatoxins poisoning.

CONCLUSIONS

In summary, biocompatible ZnO NPs have successfully been prepared using from the leaves of lemongrass using green chemistry approach. The present biosynthetic method is very handy, quick, easily reproducible, and economically viable and can easily be scaled up for mass production. Based on the obtained results, it is concluded that ZnO NPs possess an inhibitory effect on the growth of *Aspergillus flavus* along with its aflatoxins production. So, ZnO NPs has the potential to be used in the plant protection and as a preservative for safe storage of food commodities to prevent *A*. *flavus* contamination and aflatoxins poisoning in coming future.

CONFLICT OF INTEREST

The authors declare that there is no conflict of interests regarding the publication of this manuscript.

REFERENCES

[1] Mishra A., Dubey N., (1994), Evaluation of some essential oils for their toxicity against fungi causing deterioration of stored food commodities. *Appl. Environ. Microbiol.* 60: 1101–1105.

[2] Sharma A., Sharma K., (2012), Protection of maize by storage fungi and aflatoxin production using botanicals. *Indian J. Nat. Prod. Res.* 3: 215-221.

[3] Patten R. C., (1981), Aflatoxins and disease. *The Am. J. Trop. Med. Hygiene.* 30: 422–425.

[4] Williams J. H., Phillips T. D., Jolly P. E., Stiles J. K., Jolly C. M., Aggarwal D., (2004), Human aflatoxicosis in developing countries: A review of toxicology, exposure, potential health consequences, and interventions. *The Am. J. Clin. Nutrition.* 80: 1106–1122.

[5] Ma Z., Michailides T. J., (2007), Approaches for eliminating PCR inhibitors and designing PCR primers for the detection of phytopathogenic fungi. *Crop. Protect.* 26: 145–161.

[6] Jones H. C., Chancey J. C., Morton W. A., Dashek W. V., Llewellyn G. C., (1980), Toxic responses of germinating pollen and soybeans to aflatoxins. *Mycopathologia* 72: 67–73.

[7] Prakash B., Mishra P. K., Kedia A., Dwivedy A. K., Dubey N. K., (2015), Efficacy of some essential oil components as food preservatives against food contaminating molds, aflatoxin B_1 production and free radical generation. *J. Food Quality.* 38: 231–239.

[8] Jayashree T., Subramanyam C., (2000), Oxidative stress as a prerequisite for aflatoxin production by *Aspergillus parasiticus. Free Radical Biol. Med.* 29: 981–985.

[9] Shanmugam S., Xu J., Boyer C., (2015), Exploiting metalloporphyrins for selective living radical polymerization tunable over visible wavelengths. *J. Am. Chem. Soc.* 137: 9174–9185.

[10] Akther T., Khan M. S., Srinivasan H., (2018), A facile and rapid method for green synthesis of silver myco nanoparticles using endophytic fungi. *Int. J. Nano Dimens*. 9: 435-441.

[11] Palithya S., Kotakadi V. S., Pechalaneni J., Challagundla V. N., (2018), Biofabrication of silver nanoparticles by leaf extract of *Andrographis serpyllifolia* and their antimicrobial and antioxidant activity. *Int. J. Nano Dimens*. 9: 398-407.

[12] Fatema S., Shirsat M., Farooqui M., Arif P. M., (2019), Biosynthesis of silver nanoparticle using aqueous extract of *Saraca asoca* leaves, its characterization and antimicrobial activity. *Int. J. Nano Dimens*. 10: 163-168.

[13] Ghotekar S., (2019), A review on plant extract mediated biogenic synthesis of CdO nanoparticles and their recent applications. *Asian J. Green Chem.* 3: 187-200.

[14] Narasimha G., Sridevi A., Prasad B. D., Kumar B. P., (2014), Chemical synthesis of zinc oxide (ZnO) nanoparticles and their antibacterial activity against a clinical isolate *Staphylococcus aureus*. *Int. J. Nano Dimens*. 5: 337-340.

[15] Dobrucka R., Dlugaszewska J., Kaczmarek M., (2018), Cytotoxic and antimicrobial effects of biosynthesized ZnO nanoparticles using of *Chelidonium majus* extract. *Biomed. Microdevices*. 20: 5-13.

[16] Jamdagni P., Rana J. S., Khatri P., Nehra K., (2018), Comparative account of antifungal activity of green and chemically synthesized zinc oxide nanoparticles in combination with agricultural fungicides. *Int. J. Nano Dimens*. 9: 198-208.

[17] Senthilkumar N., NandhaKumar E., Priya P., Soni D., Vimalan M., Potheher I. V., (2017), Synthesis, anti-bacterial, anti-arthritic, anti-oxidant and in-vitro cytotoxicity activities of ZnO nanoparticles using leaf extract of *Tectona Grandis(L.). New J. Chem.* 41**:** 10347-10356.

[18] Mozdoori N., Safarian S., Sheibani N., (2017), Augmentation of the cytotoxic effects of zinc oxide nanoparticles by MTCP conjugation: Non-canonical apoptosis and autophagy induction in human adenocarcinoma breast cancer cell lines. *Mater. Sci. Eng. C.* 78: 949–959.

[19] Reddy A. R. N., Srividya L., (2018), Evaluation of *in vitro* cytotoxicity of zinc oxide (ZnO) nanoparticles using human cell lines. *J. Toxicol. Risk Assess*. 4: 009, 3 pages.

[20] Wang J., Gao S., Wang S., Xu Z., Wei L., (2018), Zinc oxide nanoparticles induce toxicity in CAL27 oral cancer cell lines by activating PINK1/Parkin-mediated mitophagy. *Int. J. Nanomed*. 13: 3441–3450.

[21] Sanaeimehr Z., Javadi I., Namvar F., (2018), Antiangiogenic and antiapoptotic effects of green synthesized zinc oxide nanoparticles using *Sargassum muticum* algae extraction. *Cancer Nano.* 9: 3, 16 pages.

[22] Rittner M. N., (2002), Nanostructured materials. *Am. Ceram. Soc. Bull*. 81: 33–36.

[23] Mazzola L., (2003), Commercializing nanotechnology. *Nature Biotechnol.* 21: 1137–1143.

[24] Hackenberg S., Scherzed A., Harnisch W., Froelich K., Ginzkey C., Koehler C., Hagen R., Kleinsasser N., (2012), Antitumor activity of photo-stimulated zinc oxide nanoparticles combined with paclitaxel or cisplatin in HNSCC cell lines. *J. Photochem. Photobiol. B: Biol.* 114:

87–93.
[25] Guo D., Wu C., Jiang H., Li Q., Wang X., Chen B., (2008), Synergistic cytotoxic effect of different sized ZnO nanoparticles and daunorubicin against leukemia cancer cells under UV irradiation. *J. Photochem. Photobiol. B: Biol*. 93: 119–126.
[26] Kalemba D., Kunicka A., (2003), Antibacterial and antifungal properties of essential oils. *Curr. Med. Chem*. 10: 813–829.
[27] Silva Cde B., Guterres S. S., Weisheimer V., Schapoval E. E., (2008), Antifungal activity of the lemongrass oil and citral against Candida spp. *Braz. J. Infect. Dis*. 12: 63–66.
[28] Rati E., Prema V., Shantha T., (1987), Modification of Pons's method of estimating aflatoxin B_1 in corn, groundnut and groundnut cake. *J. Food Sci. Technol*. 24: 90–91.
[29] Prasad K., Jha A. K., (2009), ZnO nanoparticles: Synthesis and adsorption study. *Nat. Sci.* 1: 129–135.
[30] Jha A. K., Kumar V., Prasad K., (2011), Biosynthesis of metal and oxide nanoparticles using orange juice. *J. Bionanosci*. 5: 162–166.
[31] Prasad K., Jha A. K., (2016), Synthesis of ZnO nanoparticles from goat slaughter waste for environmental protection. *Int. J. Cur. Eng. Tech*. 6: 147–151.
[32] Jha A. K., Prasad K., (2013), Rose (*Rosa sp*.) petals assisted green synthesis of gold nanoparticles. *J. Bionanosci*. 7: 1–6.
[33] Christopher E. E., Ernest E. A., Daniel N. E., (2014), Phytochemical constituents, therapeutic applications and toxicological profile of *Cymbopogon citratus stapf* (DC) leaf extract. *J. Pharmacogn. Phytochem*. 3: 133–141.
[34] Gupta A. K., Ganjewala D., (2015), Synthesis of silver nanoparticles from *Cymbopogon flexuosus* leaves extract and their antibacterial properties. *Int. J. Plant. Sci. Ecology.* 1: 225–230.
[35] Jha A. K., Prasad K., Prasad K., Kulkarni A. R., (2009), Plant system: Nature's nanofactory. *Colloids Surf. B: Biointerf.* 73: 219–223.
[36] Shalaka A. M., Chaudhari P. R., Shidore V. B., Kamble S. P., (2011), Rapid biosynthesis of silver nanoparticles using *Cymbopogan Citratus* (lemongrass) and its antimicrobial activity. *Nano-Micro Lett*. 3: 189–194.
[37] Guzmán, D., Ruiz-Herrera J., (1997), Relationship between aflatoxin biosynthesis and sporulation in *Aspergillus parasiticus. Fungal Genet. Biol*. 21: 198–205.
[38] Hopwood D. A., (1988), The Leeuwenhoek lecture, 1987-Towards an understanding of gene switching in Streptomyces, the basis of sporulation and antibiotic production. *Proc. Royal Soc. Lond. B.* 235: 121–138.
[39] Van Rensburg S. J., Cook-Mozaffari P., Van Schalkwyk D. J., Van der Watt J. J., Vincent T. J., Purchase I. F., (1985), Hepatocellular carcinoma and dietary aflatoxin in Mozambique and Transkei. *British J. Cancer*. 51: 713–726.
[40] Doyle M. P., Marth E. H., (1978), Degradation of aflatoxin by lactoperoxidase Abbau von aflatoxin durch lactoperoxidase. *Zeitschrift für Lebensmittel-Untersuchung und Forschung.* 166: 271–273.